Energy Transfer among CP29 Chlorophylls: Calculated Förster Rates and Experimental Transient Absorption at Room Temperature

Gianfelice Cinque,* Roberta Croce,*† Alfred Holzwarth,† and Roberto Bassi*

*Dipartimento Scientifico e Tecnologico, Università degli Studi di Verona, Facoltà di Scienze, Strada LeGrazie 15, I-37134 Verona, Italy; and †Max Plank Institut fur Strahlenchemie, Mülheim am der Ruhr, Stilftstrasse 34, Germany

ABSTRACT The energy transfer rates between chlorophylls in the light harvesting complex CP29 of higher plants at room temperature were calculated ab initio according to the Förster mechanism (Förster T. 1948, *Ann. Physik.* 2:55–67). Recently, the transition moment orientation of CP29 chlorophylls was determined by differential linear dichroism and absorption spectroscopy of wild-type versus mutant proteins in which single chromophores were missing (Simonetto R., Crimi M., Sandonà D., Croce R., Cinque G., Breton J., and Bassi R. 1999. *Biochemistry.* 38:12974–12983). In this way the Q_y transition energy and chlorophyll *a*/*b* affinity of each binding site was obtained and their characteristics supported by reconstruction of steady-state linear dichroism and absorption spectra at room temperature. In this study, the spectral form of individual chlorophyll *a* and *b* ligands within the protein environment was experimentally determined, and their extinction coefficients were also used to evaluate the absolute overlap integral between donors and acceptors employing the Stepanov relation for both the emission spectrum and the Stokes shift. This information was used to calculate the time-dependent excitation redistribution among CP29 chlorophylls on solving numerically the Pauli master equation of the complex: transient absorption measurements in the (sub)picosecond time scale were simulated and compared to pump-and-probe experimental data in the Q_y region on the native CP29 at room temperature upon selective excitation of chlorophylls *b* at 640 or 650 nm. The kinetic model indicates a bidirectional excitation transfer over all CP29 chlorophylls *a* species, which is particularly rapid between the pure sites A1-A2 and A4-A5. Chlorophylls *b* in mixed sites act mostly as energy donors for chlorophylls *a*, whereas site B5 shows high and bidirectional coupling independent of the pigment hosted.

INTRODUCTION

In higher plant chloroplasts, many pigment-binding proteins are inserted into the thylakoid membrane and organized into multisubunit complexes called photosystems. Photosystems (PS) catalyze the light absorption, the use of the excitation energy in transmembrane electron transport and, finally, the ATP and NADPH synthesis. PSI and PSII are both composed of a chlorophyll *a* binding core complex surrounded by a chlorophyll *a/b*-binding antenna. A detailed understanding of energy transfer processes in antenna and reaction centers has been so far prevented by insufficient knowledge of the major parameters controlling the process, namely distances between chromophores, absorption and fluorescence energy levels and their distribution inside the photosystems, and the mutual orientation between transition dipoles. In the case of PSII light harvesting proteins (Lhcb), considerable insight has been obtained by crystallography on the major antenna complex, i.e., light-harvesting complex II (LHCII); its 3.4-Å resolution structure (Kühlbrandt et al., 1994) showed that many of the binding sites are chemically distinct and that nearest-neighbor chlorophylls (Chl) are spaced by 9 to 13 Å (center-center distance). Absorption spectra of light harvesting complex (LHC) proteins display a markedly heterogeneous broadening in the 630–685 nm range. From optical spectroscopic measurements, 8 to 11 spectral forms have been identified with reasonable certainty (Hemelijk et al., 1992), and the number of bound Chls per monomer is in the 8–14 range (Kühlbrandt and Wang, 1991; Kühlbrandt et al., 1994; Dainese and Bassi, 1991), suggesting that the spectral heterogeneity depends on the different protein environments in which individual chromophores are located. Based on LHCII structure, mutation analysis of chlorophyll binding sites has become possible, leading to the construction of mutant proteins lacking individual chromophores that were used for determination of the absorption energy levels for each Chl in Lhcb1 and Lhcb4 gene products, namely LHCII and CP29 proteins (Bassi et al., 1999; Remelli et al., 1999). The orientation of electronic transition dipole moments of the chromophores cannot yet be obtained from structural data. Here again the recombinant CP29 system has been used for the experimental analysis of the orientation of the transition moments of individual Chl molecules (Simonetto et al., 1999). CP29 is thus the first LHC protein for which all the major parameters involved in the excitation energy transfer have been determined. In this work we have integrated the recently obtained knowledge on CP29 for calculation of excitation energy transfer rates between individual chromophores in the pigment-protein based on Förster mechanism. The above information allowed us to analytically calculate the time-dependent excitation redistribution among CP29 chlorophylls by solving numerically the Pauli master equation of the complex. Computer simulation of

Received for publication 28 January 2000 and in final form 5 July 2000.

Address reprint requests to Roberto Bassi, Dipartimento Scientifico e Tecnologico, Università degli Studi di Verona, Facoltà di Scienze MM.FF.NN., Strada LeGrazie 15, I-37134 Verona, Italy. Tel.: +39-045-802-7916; Fax: +39-045-802-7929; E-mail: bassi@sci.univr.it.

© 2000 by the Biophysical Society

0006-3495/00/10/1706/12 $2.00

transient absorption spectroscopy in the (sub)picosecond time scale are also presented and discussed in comparison to pump-and-probe experimental data on the native CP29 at room temperature (RT) in the Q_y region using selective excitation of Chls *b* at 640 an 650 nm.

MATERIALS AND METHODS

Sample preparation

Native CP29 protein was purified from maize PSII membranes as already described in Croce et al. (1996). Recombinant CP29 was obtained by in vitro reconstitution of the apoprotein overexpressed in *Escherichia coli* with purified pigments (Giuffra et al., 1996). Recombinant Lhcb4 and Lhcb1 proteins carrying mutation in individual chlorophyll binding residues were produced according to Bassi et al. (1999) and Remelli et al. (1999).

For stoichiometric (pigments/protein ratio) determination, the protein concentration was determined by the ninhidrine method (Hirs, 1967). Chlorophyll concentration was determined by the method of Porra et al. (1989). High pressure liquid chromatography analysis was performed according to Gilmore and Yamamoto (1991).

Steady-state spectroscopy

Absorption spectra were performed by using a SLM-Aminco (Rochester, NY) DW-200 Spectrophotometer. Samples were measured in 10 mM Hepes (pH 7.6), 0.06% DM, and 20% glycerol at RT. The total Chl concentration was in the order of 10 μg/ml (about 1 OD of maximum Q_y absorption). The linear dichroism (LD) spectra of the recombinant Lhcb proteins were obtained according to Haworth et al. (1982) and using samples oriented in polyacrylamide gel by the squeezing technique already described by Breton et al. (1973).

Laser system

Transient absorption was performed at RT on native CP29 upon excitation of the Chl *b* pool by a pump-and-probe laser system described elsewhere (Holzwarth and Muller, 1996). Schematically, subpicosecond excitation flashes (60 fs duration) are generated by a Ti-Sapphire laser, and successively wavelength shifted up to 640 and 653 nm with a nearly transform-limited output (about 8 nm FWHM). The super-continuum white light probe is polarized at the magic angle (54°45′) relative to the pump beam in order to exclude depolarization effects. A spectrograph/diode array system accomplishes the detection with a signal-to-noise ratio of the order of 10^5. The low photon density flux of about 10^{13} ph cm^{-2} pulse^{-1} at the repetition rate of 3 kHz avoid annihilation effects on the sample (Connelly et al., 1997).

RESULTS

Model of CP29 structure and identification of chromophores by mutagenesis

In order to calculate the Förster rates between pigments within protein complexes, the relative position of all the chromophores involved in energy transfer must be known.

This point was directly addressed by electron crystallography on LHCII, the only antenna of plant photosystem whose structure has been resolved at near atomic resolution (Kühlbrandt et al., 1994). In the case of CP29, a structural model could be inferred due to its high homology with the major antenna complex of PSII (Simonetto et al., 1999). The model structure of CP29, given in Fig. 1, illustrates the spatial organization of the Chls present in the protein. Their relative positions are summarized in Table 1 in terms of center-to-center distances (Mg to Mg atom).

The 3.4-Å resolution of the antenna protein LHCII allows definition of all the phorphyrin planes and their arrangement in space, but does not provide any distinction between Chl *a* and *b* moieties, nor information on their transition moment orientation. Recently, these parameters were determined on the basis of site-directed mutagenesis: a series of recombinant Lhcb4 and Lhcb1 apoproteins was overexpressed in bacteria after substitution of individual chlorophyll binding residues. Upon in vitro refolding (Giuffra et al., 1996), stable complexes missing specific chromophore were successfully obtained, and the biochemical analysis confirmed the correct binding of 7 Chls per mutant versus the 8 tetrapyrroles present in the wild-type (WT) protein. This approach was effective in both identifying and characterizing the chromophores bound to each site of CP29 and LHCII proteins (Bassi et al., 1999; Remelli et al., 1999).

Chlorophyll *a*/*b* absorption line shapes in Lhcb proteins

Lhcb proteins modified in order to eliminate a single Chl were also essential for determination of the energy levels in electronic transitions associated with individual chromophores by differential spectroscopy within the broad Q_y absorption band of the complex. Two special cases of re-

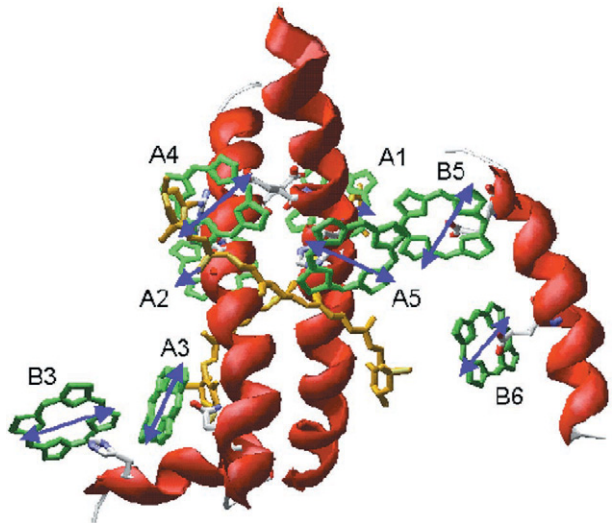

FIGURE 1 Model structure of CP29 pigment-protein complex in the membrane plane: the α-helices are in red, the chlorophylls in green with their side-chain ligands, and the chain structures of the two carotenoids identified in LHCII in orange. The Q_y transition dipole moments of the chlorophylls are in blue.

TABLE 1 Center-to-center distances (nm) between CP29 chlorophylls as conserved from LHCII crystallographic structure

Site	A2	A3	A4	A5	B5	B3	B6
A1	1.23	2.62	1.62	1.94	1.64	3.14	2.03
A2	—	1.92	1.74	2.40	2.49	2.14	2.55
A3		—	1.96	2.13	2.75	0.92	2.70
A4			—	1.27	1.75	2.52	2.69
A5				—	0.89	2.99	1.88
B5					—	3.58	1.46
B3						—	3.50

combinant CP29 and LHCII proteins lacking, respectively, one Chl *a* in site A2 of CP29 and one Chl *b* species in site A7 of LHCII were recently analyzed by differential absorption spectroscopy to their wild-types for obtaining both spectral form and molar extinction coefficient of individual Chl *a* and *b* molecules within a Lhcb environment at RT (Cinque et al., 2000). These absorption line shapes were used to reconstruct steady state spectra and also to evaluate the overlap integral of native CP29 chlorophyll protein complex.

Chlorophyll transition moment vectors

In the dipole-dipole coupling, the second determinant parameter consists in the relative orientation between the transition moment of the interacting chromophores. Recently, we determined the orientation of the Q_y transition vectors of Chls in CP29 by coupling the mutational analysis to both absorption and LD differential spectroscopy (Simonetto et al., 1999). Recombinant CP29 were oriented in a polyacrylamide gel matrix by compression and LD measured at 100 K. In this geometry (Breton et al., 1973), the proportionality between LD and absorption difference spectra (WT minus mutant) can be related to the transition dipole orientation in terms of the azimuth angle φ, with respect to the normal of the plane, of the Chl removed by point mutagenesis:

$$\mathrm{LD} = \frac{3}{2}\,\mathrm{Abs}\cdot(1 - 3\cos^2\varphi) \qquad (1)$$

Within the porphyrin planes belonging to the CP29 model structure (Fig. 1), the Q_y transition moment of bound Chls were identified by recurrence of the normalization factor from the unique proportionality constant between LD and absorption intensity over all the couples WT-mutant spectroscopically analyzed by difference.

The two remaining chromophores in site A1 and A3 were oriented via reconstruction of the steady-state LD and absorption spectra of CP29 WT at low temperature. Fig. 2, *A* and *B*, shows the results of this approach, here performed at RT, which consists in the summation of independent Chl *a* and *b* spectral forms as experimentally determined in the protein. In associating one spectral component per mutated chlorophyll site, the linear dichroic signal of each chromophore is related to its absorption counterpart via the experimental azimuth angle according to Eq. 1. From a mutant lacking chromophore A3 it was possible to locate its major Q_y contribution as the bluest transition among the Chl *a* forms at 668 nm: its dipole orientation is constrained by the negative contribution required in the LD signal at this wavelength (Fig. 2 *B*). Mutation of the A1 binding site prevented the protein refolding; however, subtraction of the difference spectra of all mutants from the WT absorption suggested the wavelength for this Q_y transition to be near

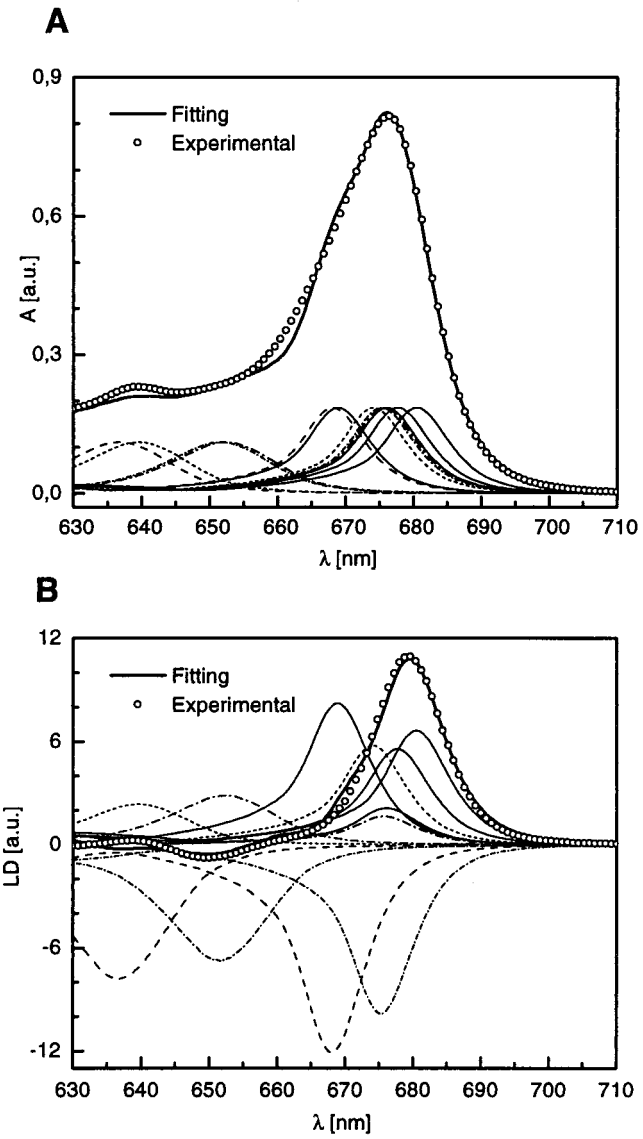

FIGURE 2 Reconstruction of absorption (*A*) and linear dichroism (*B*) spectroscopy on CP29 wild-type at RT by independent spectral forms of chlorophylls: four integer *a* forms (*continuous line*) and four *a/b* fractions (*dashed line*) of chromophores are present according to the affinities listed in Table 2, up to a total of six chlorophyll *a* and two chlorophyll *b*.

669 nm. Its orientation is determined in space by the local twofold symmetry of highly homologous domains of helices A and B in CP29 (Fig. 1) on considering the orientation of chlorophyll couples, respectively, A1-A4 and A2-A5 (Sandonà et al., 1996; Simonetto et al., 1999).

Biochemical analysis first evidenced that some binding sites in CP29 must have affinity for both Chl *a* and *b* species. Thus, mixed occupancy of sites A3, B3, A6, and B5 has been introduced to reproduce the LD intensity ratio between the overlap of Chl *a* peaks (above 660 nm) with respect to the Chl *b* ones (below 660 nm). The absorption spectrum is not sensitive to this aspect, because the overall Chl *a* and *b* contributions are weakly affected as long as the total protein stoichiometry is maintained (6 Chl *a* and 2 Chl *b*). Table 2 summarizes the main transition wavelengths, site affinities, and azimuth angles associated with the chlorophyll Q_y dipoles in the WT complex.

Förster energy transfer

Concerning the nature of the energy transfer between chlorophylls in Lhcb proteins, the Förster mechanism (Förster, 1965) was generally considered (van Grondelle et al., 1994; Jennings et al., 1996a) and here assumed in the calculations. Steady-state spectroscopy on CP29 protein indicates that the pigment binding complex is, to a large extent, weakly coupled (Zucchelli et al., 1994; Giuffra et al., 1997), although several Chl pairs could have an excitonic character. The use of incoherent energy transfer in this system seems justified through several experimental investigations (Giuffra et al., 1997; Trinkunas et al., 1997; Sandonà et al., 1998; Bassi et al., 1999). Coherent effects are, therefore, excluded from our study, and transient absorption data below the 100-fs time scale are neglected.

The energy transfer rate can be derived from the Fermi golden rule upon considering the Coulomb interaction between a donor (D) and an acceptor (A) pigment. Following Förster (1965), it may be written in terms of parameters that are experimentally more accessible, i.e.:

$$K_{\mathrm{DA}} = \frac{k^2}{\tau_{\mathrm{D}}}\left(\frac{R_0}{R_{\mathrm{DA}}}\right)^6 \qquad (2)$$

The natural lifetime of the free pigments τ_{D} constrains the time scale within an upper limit, whereas the 6th power dependence to the inverse of the pigment distance R_{DA} reflects the electric dipole-dipole interaction. The geometrical factor k^2, variable between 0 and 4, is due to the scalar product between the transition dipoles moments, μ_{D} μ_{A}, and with the distance versor R_{DA}. Since only the orientations are concerned in k^2, one can write the following relation after standard definition of unit vectors for all the quantities involved:

$$k^2 = [\hat{\mu}_{\mathrm{D}} \cdot \hat{\mu}_{\mathrm{A}} - 3(\hat{\mu} \cdot \hat{R}_{\mathrm{DA}})(\hat{\mu}_{\mathrm{A}} \cdot \hat{R}_{\mathrm{DA}})]^2 \qquad (3)$$

Table 3 summarizes this information on CP29 geometry by listing the k^2 factor between all the couples of tetrapyrroles in CP29.

In the end the so called Förster radius, R_0, accounts for the overlap between the donor fluorescence F_D, with intensity normalized to unity, and the acceptor absorbance, as molar extinction coefficient ϵ_{A}, finally integrated in the wavenumber scale (van Grondelle, 1985):

$$R_0^6 = \frac{8.785 \cdot 10^{17}}{n^4}\int \frac{F_{\mathrm{D}}\epsilon_{\mathrm{A}}}{\mathrm{v}^4}\,\mathrm{dv} \qquad [\mathrm{nm}^6] \qquad (4)$$

where n is the refractive index of the medium.

Refractive index estimation in the protein

We have based our calculation on the refractive index of the medium surrounding the xanthophylls lutein and neoxanthin located at the center of LHCII and CP29 proteins (Kühlbrandt et al., 1994; Croce et al., 1999). The absorption bands of xanthophylls in Lhcb protein complexes have been used together with the expected dependence of carotenoid spectral shift on the polarizability of the medium: in solvents, it follows a direct proportionality with the ratio $(n^2 - 1)/(n^2 + 2)$, where n is the refractive index (Andersson et al., 1991). The values of the reddest peak of lutein and neoxanthin, measured in various organic solvents, were plotted versus their polarity and linearly interpolated. In this way we

TABLE 2 Site affinities and main chlorophyll Q_y transitions obtained from reconstructing the absorption and linear dicroism spectra of CP29 wild-type at room temperature

	Chlorophyll *a*			Chlorophyll *b*		
Site	Occupancy (%)	Absorption (nm)	Azimuth (°)	Occupancy (%)	Absorption (nm)	Azimuth (°)
A1	100	668.8	86	—	—	—
A2	100	680.4	75	—	—	—
A3	70	668.0	27	30	636.8	23
A4	100	676.0	60	—	—	—
A5	100	677.6	71	—	—	—
B5	60	675.2	32	40	651.6	27
B3	30	674.0	71	70	639.6	65
B6	40	675.6	59	60	652.4	68

Also shown is the azimuth angle according to Simonetto et al. (1999).

TABLE 3 Geometrical factor k^2 relating in pairs the Q_y transition moments of all the chlorophylls in native CP29 complex

Site		A2	A3	A3	A4	A5	B5	B5	B3	B3	B6	B6
	Chl	*a*	*a*	*b*	*a*	*a*	*a*	*b*	*a*	*b*	*a*	*b*
A1	*a*	**1.66**	1.14	0.92	0.76	0.76	0.06	0.03	1.06	1.13	0.60	0.34
A2	*a*		**1.91**	**1.58**	**1.28**	0.67	0.11	0.11	**1.82**	**2.03**	0.67	0.56
A3	*a*				**2.28**	0.13	0.47	0.23	0.03	0.05	0.00	0.02
A3	*b*				**2.36**	0.22	0.58	0.29	0.00	0.00	0.02	0.09
A4	*a*					0.59	0.50	0.81	**1.48**	**1.99**	0.05	0.01
A5	*a*						0.62	0.44	0.00	0.04	0.66	1.14
B5	*a*								**2.10**	**2.00**	0.20	0.52
B5	*b*								**1.58**	**1.43**	0.16	0.47
B3	*a*										1.02	**1.19**
B3	*b*										1.03	**1.24**

Terms with the highest amplitude are in bold.

obtained $n = 1.54$ for lutein and $n = 1.56$ for neoxanthin in LHCII, based on their reddest absorption peak, respectively, at 495 nm and 488 nm (Croce et al., 1999). The slightly different protein environment can explain the small differences obtained. For calculations we then used the average value of the refractive index, i.e., $n = 1.55$, as revealed by carotenoids inside the protein.

Numerical overlap integral

The overlap integral between each D-A couple from the Chl complex pool was numerically calculated on the basis of the Q_y optical transition (wavelength of the main absorption) previously determined by site-directed mutagenesis and differential spectroscopy on CP29 proteins (Simonetto et al., 1999). In the same way, the extinction coefficient and the spectral form of both Chls, *a* and *b*, were experimentally determined (Cinque et al., 2000), and their fluorescence emission within the protein environment was derived by applying the Stepanov relation to the absorption data (Stepanov, 1957). This procedure also provides the value of the Stokes shift (about 2 nm, in the case of Chl *a*) used to determine the emission wavelength of all the chromophores in the complex. As an example, Fig. 3 *A* shows the experimental absorption of Chl *a* in site A2, at 680 nm, together with its emission calculated according to Stepanov. In Fig. 3 *B*, the numerical overlap integration is shown between Chls *a*, Chls *b* and from Chl *b* emission to Chl *a* absorption. The acceptor chromophores have absorption spectra as experimentally determined in Cinque et al. (2000), that is, with main Q_y peak at 680 and 650 nm respectively, but on varying the fluorescence wavelength of the donor molecule. Notice that our calculation of the Förster radius gives absolute values, and the plot shown in Fig. 3 *B* refers to the vacuum case ($n = 1$). Similar calculation was performed for all chromophores in CP29, including the overlap integral from Chl *a* to Chl *b* in mixed sites (data not shown).

Förster rates in CP29

Due to the presence of four mixed sites, with different affinity to the two Chl species *a* and *b*, and 4 pure chlorophyll *a* sites in the antenna CP29, 16 distinct configurations of the wild-type pigment-protein complex are allowed. Table 4 summarizes these possibilities, and the probability of each configuration is directly given by the product of the occupancy of all the mixed sites (independent probabilities). As a consequence, the Förster rates between CP29 Chls can be organized in a 12×12 element matrix with donor sites on rows and acceptors on columns: such a matrix is shown in Table 5, whose elements must be read from row to column because of the nonsymmetrical character of the matrix.

The evolution of chlorophyll excited states in CP29 complex can be formally represented by the set of coupled rate equations, collectively known as the (Pauli) master equation (Pearlstein, 1982; van Grondelle, 1985):

$$\frac{dp_i(t)}{dt} = \sum_j p_j(t) \cdot K_{ji} - p_i(t) \cdot \sum_j (K_{ij} + K_{diss}) \qquad (5)$$

These equations control the evolution of the time-dependent probability $p_i(t)$ that excitation resides on the i^{th} chromophore in terms of Förster transfer rates K_{ij} with respect to any other j^{th} pigment and from some initial condition $p_i(t = 0)$. The term K_{diss} accounts for dissipative processes in the energy transfer including any effects, e.g., internal conversion, that lead to a loss of chromophore excitation (see the Discussion for parameter evaluation). Due to the differentiation of chlorophyll Q_y transitions within the protein complex, the excitation dynamics can be investigated by observing the downhill energy flow from Chls *b* to *a* and the excited state equilibration.

For comparison with experimental measurements of transient absorption on CP29 upon selective excitation of the two Chl *b* subbands, around 650 and 640 nm, within the ensemble of CP29 configurations we considered the occu-

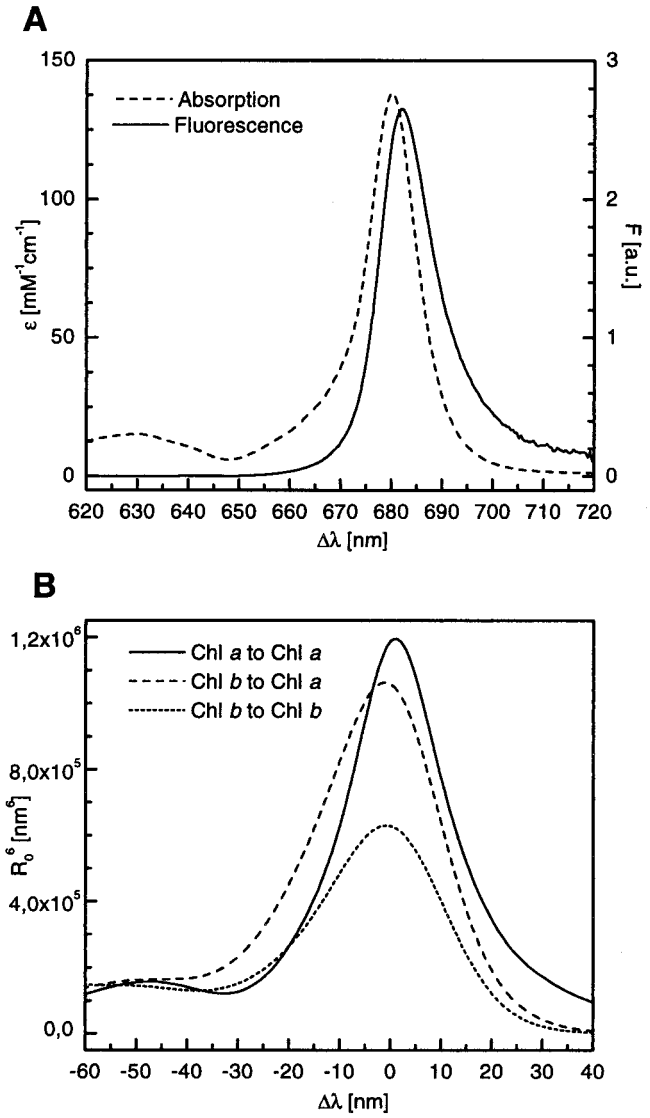

FIGURE 3 (*A*) The experimental absorption spectrum of chlorophyll *a* within Lhcb protein together with its calculated emission according to the Stepanov relation. The Stokes shift is about 2 nm. (*B*) The numerical overlap integral, in terms of the Förster radius, between chlorophylls *a-a*, *b-a*, and *b-b* as function of the donor-acceptor wavelength; the chlorophyll *a* absorption peak is at 680 nm, whereas the chlorophyll *b* absorption peak is at 650 nm.

pancy of the mixed sites, B5+B6 and A3+B3, respectively, only by Chl *b* species. These configurations are highlighted in Table 4 by bold and bold italic letters. Their probabilities were renormalized by setting the overall occurrence of either selection group 11 + 12 + 15 + 16 or 6 + 8+14 + 16 equal to 1. Within these groups, the relative probabilities can be still estimated as ratio of configuration values in Table 4.

The numerical solution of the rate equations in the finite difference scheme is straightforward by the Euler method (Press et al., 1986); for error control, conservation with time of the total excitation was used. The excitation probability was integrated on all the chromophores and checked at each time step by taking into account the fraction lost by dissipation. The time resolved differential absorption of the complex in the 620–720 nm range was simulated by "dressing" the CP29 Q_y transitions with the steady-state spectral forms of Chl *a* and *b* as determined in Lhcb proteins (Cinque et al., 2000): in the simulated spectrum, each absorption band is weighted by the time-dependent excitation probability of the corresponding chromophore.

Transient absorption measurements on native CP29

Femtosecond transient absorption measurements have been performed on native CP29 at RT by the pump-and-probe technique at the two wavelengths of main Chl *b* absorption, namely 640 and 653 nm. Laser pulses of 60 fs duration and nearly transform limited in wavelength width, about 8 nm wide, cover almost completely the main peak of individual Chl *b* forms. In Fig. 4 *A*, the experimental difference between absorption at equilibrium and over various time intervals between pump at 653 nm and probe is shown, and in Fig. 4 *B* the corresponding simulations are given for the same time delays after excitation ($t = 0$) of the Chl *b* species. It is evident from Fig. 4 that the experimentally observed energy flow from Chl *b* downward to Chl *a* species is nicely reproduced both in terms of the overall rate and spectral shape in the simulations. A value of 1.55 for the refractive index, the only free parameter in all the calculations, has been here used. The signal overestimation below 640 nm in Fig. 4 *B* can be attributed to chlorophyll *a* vibrational transitions, naturally included by using steady-state spectral forms; in transient experiments they disappear 200 fs after excitation through ultra-fast thermal relaxation. For completeness, in Fig. 5 *A* we also present the experimental data on the native CP29 upon excitation at 640 nm and the corresponding simulations in Fig. 5 *B*. In this case the estimated transfer rate of excitation from Chl *b* pool toward Chl *a* pool is about 7 times slower than measured.

The overall conclusion concerning the site-to-site kinetics of CP29 chlorophyll complex is schematized in Fig. 6. The pure Chl *a* sites form an internal "kernel," which is rapidly equilibrated due to bidirectional excitation transfer. According to our calculations, the most rapid transfer steps take place within the twofold symmetry-related couples of chromophores A1-A2 and A4-A5, whereas their intercrossing rates are smaller but certainly effective. All the other sites are mixed and surround the central kernel. They are less strongly interacting and this is almost exclusively to their two or three closest neighbors. When Chl *a* species populate such mixed sites the whole CP29 chlorophyll system is rapidly equilibrated, since an effective and bidirectional energy pathway is present. Conversely, mixed sites filled by Chls *b* act essentially as energy donors; therefore, excitation

TABLE 4 Allowed configurations for native CP29 pigment protein complex on considering the mixed site occupancies by chlorophylls *a* or *b*

Configuration	*1*	*2*	*3*	*4*	*5*	***6***	*7*	***8***	*9*	*10*	**11**	**12**	*13*	***14***	**15**	***16***
Chl in A3	*a*	*b*	*a*	*b*	*a*	***b***	*a*	***b***	*a*	*b*	**a**	**b**	*a*	***b***	**a**	***b***
Chl in B5	*a*	*a*	*b*	*b*	*a*	***a***	*b*	***b***	*a*	*a*	**b**	**b**	*a*	***a***	**b**	***b***
Chl in B3	*a*	*a*	*a*	*a*	*b*	***b***	*b*	***b***	*a*	*a*	**a**	**a**	*b*	***b***	**b**	***b***
Chl in B6	*a*	*a*	*a*	*a*	*a*	***a***	*a*	***a***	*b*	*b*	**b**	**b**	*b*	***b***	**b**	***b***
A3 Occupancy	*0.7*	*0.3*	*0.7*	*0.3*	*0.7*	***0.3***	*0.7*	***0.3***	*0.7*	*0.3*	**0.7**	**0.3**	*0.7*	***0.3***	**0.7**	***0.3***
B5 Occupancy	*0.6*	*0.6*	*0.4*	*0.4*	*0.6*	***0.6***	*0.4*	***0.4***	*0.6*	*0.6*	**0.4**	**0.4**	*0.6*	***0.6***	**0.4**	***0.4***
B3 Occupancy	*0.3*	*0.3*	*0.3*	*0.3*	*0.7*	***0.7***	*0.7*	***0.7***	*0.3*	*0.3*	**0.3**	**0.3**	*0.7*	***0.7***	**0.7**	***0.7***
B6 Occupancy	*0.4*	*0.4*	*0.4*	*0.4*	*0.4*	***0.4***	*0.4*	***0.4***	*0.6*	*0.6*	**0.6**	**0.6**	*0.6*	***0.6***	**0.6**	***0.6***
Probability	*0.05*	*0.02*	*0.03*	*0.01*	*0.12*	***0.05***	*0.08*	***0.03***	*0.08*	*0.03*	**0.05**	**0.02**	*0.18*	***0.08***	**0.12**	***0.05***

The product of fractional site affinities ensures the final probability per configuration. In bold type are the configurations experimentally tested by time-resolved laser spectroscopy, in plain text those for 640 nm, and in italics those for 653 nm. The last configuration (16, last column) is in common to both.

flow preferentially toward the central kernel. The exception is given by site B5, since it shows the highest transfer rates and is always equilibrated with the rest whatever the pigment hosted.

DISCUSSION

It was previously demonstrated by steady state spectroscopy on both native and recombinant CP29 that chlorophyll-protein interactions dominate other inter-chromophore effects in the Q_y optical region (Giuffra et al., 1997). As a consequence, the spectral heterogeneity both in absorption and LD of CP29 WT could be accounted for in terms of independent spectral bands, equal in number to the chromophores determined by protein stoichiometry (Simonetto et al., 1999). In this study we extended such an approach at RT upon using the Chls *a and b* absorption forms Lhcb protein environment from Cinque et al. (2000). These are very similar in shape to the pure pigment absorption in organic solvents in the Q_y and Q_x region.

In Fig. 2, both the absorption (*A*) and the LD spectra (*B*) of the WT complex CP29 are reconstructed by the same set of individual Chl optical subbands. Chlorophyll site interactions were only described through a wavelength shift of the spectral forms (Zucchelli et al., 1994; Jennings et al., 1996b), therefore the remaining discrepancies between reconstruction and experiment in Fig. 2 may be due to local environment inhomogeneities from site to site or, possibly, to minor excitonic interactions between chromophores.

Here, the wavelength of the main Q_y transitions were once again derived from the same series of CP29 mutants already studied at low temperature but by performing the absorption difference analysis at RT. In comparison with the 100 K data, the present results of Table 2 reveal a general red shift of the chromophore transitions at RT, except for Chl *a* in site A1, which essentially remains constant in wavelength of absorption. The order in the set of chlorophyll Q_y transition energies is maintained with temperature, with the A2 being the most red-shifted form while Chl in sites A1 and A3 appears to be the most blue-shifted among

TABLE 5 Förster rates between chlorophylls of the native CP29 complex at room temperature

Site		A1	A2	A3	A3	A4	A5	B5	B5	B3	B3	B6	B6
	Chl	*a*	*a*	*a*	*b*	*a*	*a*	*a*	*b*	*a*	*b*	*a*	*b*
A1	a	—	**14.18**	0.09	0.00	**1.49**	***0.47***	0.06	0.00	0.01	0.00	***0.12***	0.02
A2	a	**5.12**	—	***0.25***	0.00	**1.30**	***0.11***	0.01	0.00	***0.13***	0.00	0.03	0.00
A3	a	0.09	**0.76**	—	—	**0.97**	0.03	0.02	0.00	***0.44***	0.02	0.00	0.00
A3	b	0.01	0.07	—	—	0.09	0.01	0.00	0.00	0.00	0.01	0.00	0.00
A4	a	**0.81**	**1.86**	***0.48***	0.00	—	**5.64**	***0.39***	0.02	0.06	0.00	0.00	0.00
A5	a	***0.22***	***0.14***	0.01	0.00	**4.95**	—	**24.79**	***0.42***	0.00	0.00	***0.21***	0.02
B5	a	0.04	0.01	0.01	0.00	***0.41***	**30.22**	—	—	0.01	0.00	***0.19***	0.04
B5	b	0.01	0.00	0.00	0.00	***0.18***	**5.16**	—	—	0.00	0.00	0.08	***0.61***
B3	a	0.01	***0.22***	***0.26***	0.00	0.07	0.00	0.01	0.00	—	—	0.00	0.00
B3	b	0.01	***0.11***	***0.42***	0.01	0.04	0.00	0.00	0.00	—	—	0.00	0.01
B6	a	0.07	0.04	0.00	0.00	0.00	***0.24***	***0.19***	0.00	0.00	0.00	—	—
B6	b	0.07	0.02	0.00	0.00	0.00	***0.24***	***0.35***	***0.32***	0.00	0.00	—	—

Expressed in ps^{-1} (row to column matrix). The leading elements are in bold, and other secondary but significant terms are italicized.

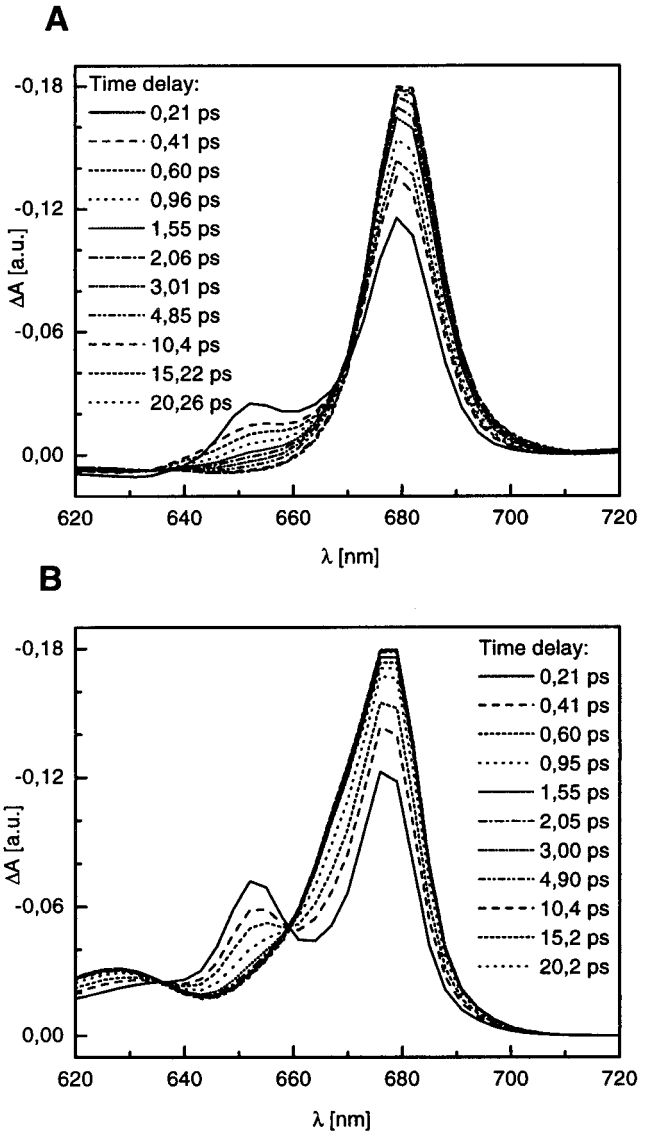

FIGURE 4 (*A*) Experimental transient absorption spectroscopy of native CP29 at RT upon excitation of chlorophyll *b* at 653 nm. (*B*) Simulated differential absorption calculated according to Förster transfer between chlorophylls; different lines distinguish time delays between pump and probe.

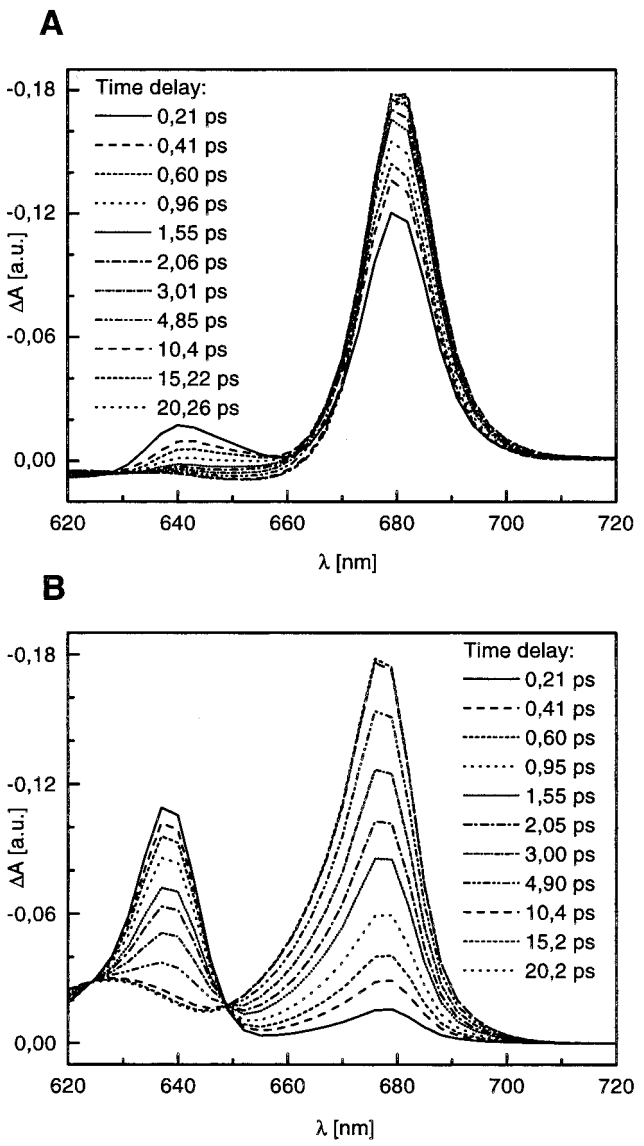

FIGURE 5 (*A*) Experimental transient absorption spectroscopy of native CP29 at RT upon excitation of chlorophyll *b* at 640 nm. (*B*) Simulated differential absorption calculated according to Förster transfer between chlorophylls. Different lines distinguish time delays between pump and probe.

Chl *a* chromophores (see Fig. 2 *A*). In employing Eq. 1 for the Q_y band polarization, orientation of Chl transition moments and their site affinities determined in previous studies were used (Simonetto et al., 1999; Bassi et al., 1999). The smallest azimuth angles in Table 2 correspond to the negative contributions in the LD reconstruction due to the mixed sites A3 and B5 in Fig. 2 *B*. We stress the point that the specificity of the peripheral sites in the antenna CP29 (Fig. 1) to bind either Chl *a* or *b* was first demonstrated and quantified by biochemical characterization of recombinant proteins (Bassi et al., 1999) independent of spectroscopic evidence.

In the pairwise excitation exchange among chromophores, the energy matching between donor and acceptor is accounted through the overlap integral. The Förster radius in Eq. 4 was calculated in the wavenumber scale from 13,000 to 17,000 cm^{-1} in steps of 20 cm^{-1} by numerical integration of experimental Chl *a/b* absorptions in Lhcb proteins, as deconvoluted into 5 Gaussians below 18000 cm^{-1} by Cinque et al. (2000), and emission spectrum calculated according to Stepanov (Fig. 3 *A*). Better than a fitting by several forms, the fluorescence emission was accurately reproduced by the mirror image on using the two reddest Gaussians of the absorption fitting. Notice that

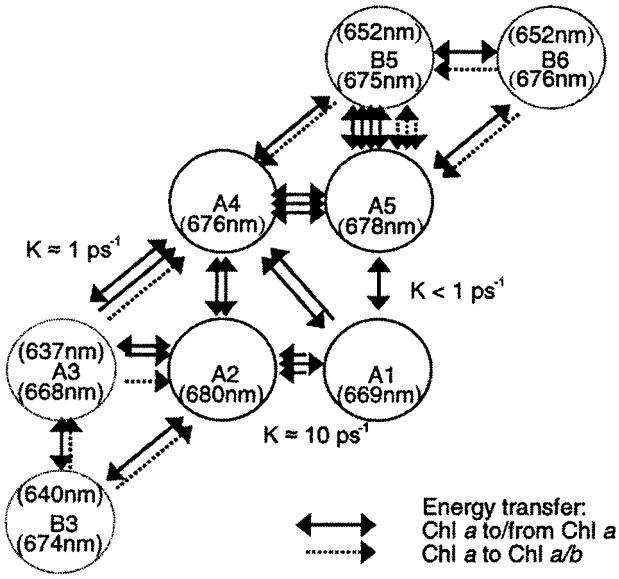

FIGURE 6 Block diagram of the excitation energy pathways in native CP29 at RT. Full line circles indicate pure chlorophyll *a* sites, and the mixed sites are dotted. The same convention applies to the energy directions, with full arrows for transfers between chlorophylls *a* and dotted lines used between chlorophylls *b* or different species.

Stepanov's law could be applied for chlorophyll emission since thermal equilibration is rapidly attained in the pigment-protein complexes used for differential absorption, i.e., in both recombinant and native LHCII/CP29 spectra (Giuffra et al., 1997; Remelli et al., 1999). For integration, all the CP29 chlorophylls were considered in couples and their individual absorption bands were only spectrally shifted to agree with CP29 Q_y transition wavelengths in Table 2. It is worth noting that the Stokes shift value of 2 nm (40 cm^{-1}), found by applying the Stepanov rule to our experimental Chl *a* form, is in good agreement with data from hole burning in LHC proteins by Gillie et al. (1989). In fact, a Huang-Rhys factor of $S = 0.8$ in linear electron-phonon coupling and mean protein mode of $\nu = 22$ cm^{-1} gives approximately $2S\nu = 35$ cm^{-1} (Jennings et al., 1996b).

In Fig. 3 *B*, the Förster radius between Chls *a* in CP29 is quite similar to the main overlap peak obtained via analytical integration by Shipman and Housmann (1979); referring to the maximum, here the intensity of the secondary peak is more than halved because of the relative enhancement of the electronic absorption in our Lhcb Chl form. The overlap integral recently estimated in LHCII and CP29 pigment protein complexes at 77 K was obviously narrower in the main band but, by employing the analytical method extension of Jean et al. (1988), any secondary features were neglected (Gradinaru et al., 1998, 1999). Concerning the Chl *b* overlap integral (Fig. 3 *B*), to our knowledge this is the first report in which an estimation is performed on the basis of an experimentally determined Chl *b* spectral form.

In the frame of Förster theory, the transfer rates between the Chls present in CP29 have been computed from Q_y transition data. The pairwise interaction of 4 pure plus 4 mixed sites times 2 chromophore moieties determined the 12×12 transfer rates arranged by matrix form in Table 5. Its nondiagonal character reflects the irreversibility in the energy flow over the physical system; indeed, the ratio between each forward and backward Förster rate correctly satisfies the Boltzmann probability of crossing the free energy gap between donor and acceptor excited levels at thermal equilibrium and RT (van Grondelle, 1985). A crucial point is the evidence of some large matrix elements in Table 5 as a result of our calculations, which suggest a strong coupling between some chromophores in the CP29 antenna. This, however, does not contradict the theoretical frame we used, because Kenkre and Knox (1974) demonstrated that the excitation transfer can be correctly described by a Förster approximation even in this case.

The value of the refractive index to be used in modeling the pigment protein complex is still an open question. In principle, it depends on the local polarizability of each pigment site, and in fact its variation within the protein drives the differentiation of the optical transitions of the chromophores in the visible range (Borisov, 1996; Seely and Jensen, 1965). In our calculation, however, we followed the idea of considering an average over all the protein chromophores in order to account phenomenologically for the screening effects in the pairwise interaction potential between the Chls. The mean value of the protein refractive index as cross-spanned by the carotenoids is $n = 1.55$, and it correctly reproduces the time scale in the transient absorption simulations. Furthermore, it is well within the range of values quoted in the literature for similar evaluations of Chl coupling within antenna proteins (Trinkunas et al., 1997; Gradinaru et al., 1998, 1999).

Data in Table 5 are drawn for clarity in the kinetic model of Fig. 6; the leading terms are all due to excitation exchanges among Chls *a*, in the order between sites B5-A5, A2-A1, and finally A5-A4. Of the same size is the unique strong energy transfer between a Chl *b* and a Chl *a*, i.e., from site B5 toward A5 (mixed to pure site). This large rate is mainly responsible for the rapid energy transfer experimentally observed upon excitation at 640 nm and fairly simulated on native CP29 complex. The large energy separation and Stokes shift strongly decreases the reverse transfer rate in this pair. Secondary energy exchanges take place between three Chl *a* pairs, namely between sites A1 and A5, A1 and A2, and A3 and A4. Thus, site A4 seems to play a pivotal role for equilibration among the low energy chromophores in CP29, i.e., the Chl *a* central kernel of the complex. With respect to the Chl *a* kernel, two groups of chromophores are symmetrically located on, respectively, the helix C domain (sites B5 and B6) and the helix D domain (sites A3 and B3). Although site B5 shows a strong exchange with the group of pure Chl *a* sites (via site A5),

energy transfer rate toward A2 from mixed site A3 is favored only when the former is filled by Chl *a* (Fig. 6). It is worth mentioning that the weakness of the Chl *b* coupling to A2 cannot explain the experimental data on native CP29 upon excitation at 640 nm, at least using the dipole-dipole coupling and data presently available on CP29.

Among the 2^4 configurations of native CP29, obtained from 2 chromophore species and 4 mixed sites independently filled, we restricted our calculation to the 7 cases indicated in bold in Table 4 in modeling the transient behavior of absorption changes. The corresponding transfer rates were considered on solving the master equation (Eq. 5) under initial conditions of equal excitation of either sites A3 and B3 (absorption at 640 nm) or B5 and B6 (absorption at 653 nm). Numerically, a time step of 50 fs ensured an overall error of $<0.1\%$ after 20 ps. The dissipative term K_{diss} in Eq. 5 was set as the inverse time constant of the experimental Chl *a* de-excitation; after integration of the transient absorption spectrum, a value of about 3 ns was estimated by fitting the total area decay beyond 10 ps via a simple exponential curve.

Experimentally, by transient spectroscopy we investigated those CP29 complexes which host only Chls *b* in the mixed sites of one lateral "wing" in the block diagram of Fig. 6. Due to the clear separation between the wings, these tests are practically independent on the species present in the mixed sites at the opposite side. The transient absorption simulations (Fig. 4 *B*) of native CP29 complex after initial excitation at 653 nm are in good agreement with the actual data (Fig. 4 *A*): in particular, the rise time of the differential absorption signal above 660 nm is well reproduced in terms of progressive filling of the Chl *a* excited states. The concomitant depletion with time of the Chl *b* excited levels, i.e., the signal decay below 660 nm, is also present, but a direct comparison with the experimental signal is hampered by the long blue tail of vibrational levels introduced in the simulation by the steady-state Chl *a* forms. We did not attempt any shaping of the Chl forms in transient absorption to avoid arbitrariness in the simulations: it is worth mentioning that no adjusting parameters are present through all the calculations except for the refractive index, used as a time scaling factor, which, however, is constrained by the value of 1.55 based on the xanthophyll absorption peaks. On the other hand, data for the transient absorption on native CP29 after excitation at 640 nm (Fig. 5 *A*) are markedly different from our energy modeling according to Förster (Fig. 5 *B*). A possible explanation arises from considering the subband of Chl *a* vibrational overtones, observable below 650 nm in Fig. 5 *B*, and that are certainly excited by the broad laser pulse at 640 nm. Vibrational relaxation to the low-lying electronic transitions may mimic an excitation transfer toward Chls *a* much faster than Förster rate. Vibrational relaxation can effectively account for the rapidity of the transient absorption experimentally observed by laser excitation at 640 nm, behavior which is comparable in time scale to the other data at 653 nm. In order to check other possibilities, we also considered the case that the transition moment of Chl A3 could have been misfitted in previous work (Simonetto et al., 1999). From the CP29 energy pathway in Fig. 6 it is evident how A3 is the bottleneck in the excitation flow from the bluest Chl *b*, namely B3 and A3 itself; therefore, a different orientation of Chl A3 could influence the transient behavior of the complex upon excitation at 640 nm. Four orientations are allowed for the Q_y transition vector of Chl A3 in CP29 assuming conservation of the porphyrin plane experimentally determined in the homologous protein LHCII (Kühlbrandt et al., 1994) and considering only possibilities leading to the phytol chain pointing inward to the lipid bilayer (Simonetto et al., 1999). However, calculation of the transfer rates in all these cases demonstrates only a dramatic increase of the coupling between sites B3 and A3 without any improvement of the exchange rate toward the Chl *a* kernel via A2 or A4. Furthermore, in Table 3 the geometrical factor k^2 relating A3 Q_y transition vector to both A2 and A4 is already among the highest values, and only a factor of 2 could be ideally gained in transfer by juxtaposition of the A3 orientation.

Whether the Förster mechanism is only partly responsible for the transient absorption decay with time around 640 nm and simultaneous increase above 660 nm cannot be discounted. Certainly, it is not fully effective because of Chl A3 and its low transfer rates in Table 5. Note that this makes the CP29 excitation pathway of Fig. 6 asymmetrical in the two "wings" of mixed sites when considering the coupling of the Chls *b* in sites A3 and B5 with respect to the pure Chl *a* kernel. Interestingly, the difference in behavior of these crucial chromophores seems due to a factor of 2 in the ratio between their distances to the closest neighbors, namely B5 toward A5 and A3 toward A2 (or A4), the effect of this distance factor is strongly enhanced through the R^{-6} law expected in a dipole-dipole interaction. Thus, the lower transfer from the bluest Chls *b* ($K \approx 1\ ps^{-1}$ downward Chls *a*) with respect to that of the reddest Chl *b* in site B5 ($K \approx 10\ ps^{-1}$) seems to be a structural feature in the kinetic model of CP29, at least if Coulomb coupling is considered. The energy equilibration over all chromophores, which is essential for CP29 light harvesting function, is, however, guaranteed, as is evident from the flow diagram of Fig. 6 where, possibly, vibrational relaxation operates as a parallel mechanism to improve the transfer of light absorbed at highest energy in the Q_y region.

Apart from a different definition of the Q_y transition in the porphyrin plane, both Chl *b* absorption energies and orientation of all CP29 chromophores obtained by Gradinaru et al. (1999) via a study of transient absorption on CP29 at 77 K are very similar to the present determination, following Simonetto et al. (1999), except for chromophore A3. Neglecting complications due to mixed sites, it is worth mentioning that they could not univocally assign the transition moment of this Chl by studying CP29 excited state

dynamics upon laser excitation at 640 and 650 nm and in the Förster theoretical frame. This is an interesting point whose implications in the function of CP29 should be experimentally tested in greater detail. Direct validation of CP29 complex structure with distances and orientations of its Chls, as well as elucidation of carotenoid positioning, are required. A step forward in the knowledge of the minor antenna CP29 as a widely studied model system of the Lhcb family is possible through determination of its actual structure at high resolution after protein crystallization. Alternatively, the well established techniques of molecular biology applied on gene sequences of both Lhcb1 and Lhcb4 have nowadays demonstrated the feasibility of chimeric LHCII and CP29 proteins: upon in vitro refolding, they should permit the study of separate domains of the pigment-protein complexes also in conjunction with the single site mutagenesis approach already developed.

CONCLUSIONS

In this study we have calculated the excitation energy transfer rates between individual chlorophyll sites in the higher plant light harvesting protein CP29 by an *ab initio* approach based on the relevant parameters for Förster energy transfer (Förster, 1965) as determined by electron crystallography (Kühlbrandt et al., 1994) and site-directed mutagenesis coupled to absorption and polarized spectroscopy (Bassi et al., 1999; Remelli et al., 1999; Simonetto et al., 1999). The resulting data have been used to simulate transient absorption spectra with subpicosecond resolution upon selective excitation of two different protein domains carrying 640 and 650 nm absorbing Chl *b* chromophores. Upon 650 nm excitation, calculations closely fit experimental data in both time dependence of excited state distribution and spectral behavior, thus providing *a posteriori* verification of the correctness of the spectral properties of individual chromophores as determined in previous work (Bassi et al., 1999; Remelli et. al., 1999, Simonetto et al., 1999). In this context, it is interesting to note that calculated transient absorption spectra upon 640 nm excitation indicated a slower energy transfer rate from the A3 and B3 sites to the Chl *a* kernel with respect to the experimental observations. We propose that the discrepancy is due to the direct excitation of vibrational Chl *a* subbands by the 640 $\pm$ 4 nm laser excitation. The schema of Fig. 6 clearly shows that CP29 chromophores are clustered into three domains. The major one, organized around the twofold symmetrical helix A-helix B cross, is composed of Chl *a* chromophores only, whereas the remaining two are composed of both Chl *a* and Chl *b* and are located in the helix C domain and the helix D domain, respectively. Although the central cluster is expected to be conserved in all Lhcb proteins, the peripheral domains are clearly different in both the number of sites and spectral properties of the component chromophores, as shown in the case of major LHCII complex (Remelli et al., 1999). It is, therefore, to be expected that significant changes in the pathway of energy transfer with respect to CP29 might be recognized. These might be the basis for understanding the specific role of each LHC protein in the photosynthetic machinery.

Special thanks to M. Muller for sharing the transient absorption data on native CP29 and to J. Breton for the linear dichroism measurements on CP29 wild-type. We also acknowledge D. Gulen and R. Jennings for critically reading the manuscript. This work was supported by MURST and CNR target project on biotechnology.

REFERENCES

Andersson, P. O., T. Gillbro, L. Ferguson, and R. J. Cogdell. 1991. Absorption spectral shift of carotenoids related to medium polarizability. *Photochem. Photobiol.* 54:353–360.

Bassi, R., R. Croce, D. Cugini, and D. Sandonà. 1999. Mutational analysis of higher plant antenna protein provides identification of chromophores bound into multiple sites. *Proc. Natl. Acad. Sci. USA.* 96:10056–10061.

Borisov, A. Y. 1996. Specific features of excitation migration in photosynthesis. *In* Light as an Energy Source and Information Carrier in Plant Physiology. R. C. Jennings, G. Zucchelli, F. Ghetti, and G. Colombetti, editors. NATO ASI Series A 287:31–40. Plenum Press, New York.

Breton, J., M. Michel-Villaz, and G. Paillotin. 1973. Orientation of pigments and proteins in the photosynthetic membrane of spinach cloroplasts, a linear dichroism study. *Biochim. Biophys. Acta.* 314:42–56.

Cinque, G., R. Croce, and R. Bassi. 2000. Absorption spectra of chlorophyll a and b in Lhcb protein environment. *Photosynth. Res. special issue.* In press.

Croce, R., G. Cinque, A. Holzwarth, and R. Bassi. 2000. The Soret absorption properties of carotenoids and chlorophylls in antenna complexes of higher plants. *Photosynth. Res. special issue.* In press.

Connelly, J. P., M. G. Muller, R. Bassi, R. Croce, and A. R. Holzwarth. 1997. Femtosecond transient absorption study of carotenoid to chlorophyll energy transfer in the light harvesting complex II of photosystem II. *Biochemistry.* 36:281–287.

Croce, R., J. Breton, and R. Bassi. 1996. *Biochemistry.* 35:11142–11148.

Croce, R., R. Remelli, C. Varotto, J. Breton, and R. Bassi. 1999. The neoxantine binding sites of the major light harvesting complex (LHCII) from higher plants. *FEBS Lett.* 456:1–6.

Dainese, P., and R. Bassi. 1991. Subunit stochiometry of the cloroplast photosystem II antenna system and aggregation state of the component chlorophyll a/b binding proteins. *J. Biol. Chem.* 266:8136–8142.

Förster, T. 1948. Zwischemolekulare energiewanderung und fluoreszenz. *Ann. Physik.* 2:55–67.

Förster, T. 1965. Delocalized excitation and excitation transfer. *In* Modern Quantum Chemistry, part III. O. Sinanoslu, editor. Academic Press, New York. 93–137.

Fragata, M., B. Norden, and K. Kurucsev. 1988. Linear dichroism (250–700 nm) of chlorophyll a and pheophytine a oriented in a lamellar phase of glycerylmonooctanoate/H_2O. *Photochem. Photobiol.* 47: 133–143.

Gillie, U. K., G. J. Small, and J. H. Golbeck. 1989. Nonphotochemical hole burning of the native antenna complex of photosystem I (PSI-200). *J. Phys. Chem.* 83:1620–1627.

Gilmore, A. M., and H. Y. Yamamoto. 1991. Resolution of lutein and zeaxantin using a non-encapped likely carbon-bonded C18 HPLC column. *J. Chromatogr.* 543:137–145.

Giuffra, E., D. Cugini, R. Croce, and R. Bassi. 1996. Reconstitution and pigment-binding properties of recombinant CP29. *Eur. J. Biochem.* 238:112–120.

Giuffra, E., G. Zucchelli, D. Sandonà, R. Croce, D. Cugini, F. M. Garlaschi, R. Bassi, and R. C. Jennings. 1997. Analysis of some optical properties of native and reconstituted photosystem II antenna complex,

CP29, pigment binding sites can be occupated by chlorophyll a or chlorophyll b and determine the spectral forms. *Biochemistry.* 36: 12984–12993.

Gradinaru, C. C., S. Ozdemir, D. Gulen, I. H. M. van Stokkum, R. van Grondelle, and H. van Amerongen. 1998. The flow of excitation energy in LHCII monomers: implications for the structural model of the major plant antenna. *Biophys. J.* 75:3064–3077.

Gradinaru, C. C., A. Pascal, F. van Mourik, B. Robert, P. Horton, R. van Grondelle, and H. van Amerongen. 1999. Ultrafast evolution of the excited states in the chlorophyll a/b complex CP29 from green plants studied by energy selective pump probe spectroscopy. *Biochemistry.* 37:1143–1149.

Haworth, P., C. J. Arntzen, P. Tapie, and J. Breton. 1982. Orientation of pigments in the thylakoid membrane and in the isolated chlorophyll-protein complexes of higher plants: determination of the optimal conditions for linear dichroism measurements. *Biochim. Biophys. Acta.* 682:152–159.

Hemelrijk, P. W., S. L. S. Kwa, R. van Grondelle, and J. P. Dekker. 1992. Spectroscopic properties of LHCII, the main chlorophyll a/b protein complex from cloroplast membrane. *Biochim. Biophys. Acta.* 1098: 159–166.

Hirs, C. H. W. 1967. Detection of peptides by chemical methods. *Methods Enzymol.* 11:325–329.

Holzwarth, A., and M. Muller. 1996. Energetics and kinetics of radical pairs in reaction centers from Rhodobacter sphaeroides: a femtosecond transient absorption study. *Biochemistry.* 35:11820–11831.

Jean, J. M., C. K. Chan, and G. R. Fleming. 1988. Electronic energy transfer in photosynthetic bacterial reaction centers. *Isr. J. Chem.* 28: 169–165.

Jennings, R. C., R. Bassi, and G. Zucchelli. 1996a. Antenna structure and energy transfer in higher plant photosystems. *Topics Curr. Chem.* 177: 147–181.

Jennings, R. C., G. Zucchelli, L. Finzi, and F. M. Garlaschi. 1996b. Spectral etherogenity and energy equilibration in higher plant photosystems. *In* Light as an Energy Source and Information Carrier in Plant Physiology. R. C. Jennings, G. Zucchelli, F. Ghetti, and G. Colombetti, editors. Plenum Press, New York. 65–74.

Kenkre, V. M., and R. S. Knox. 1974. Theory of fast and slow excitation transfer rates. *Phys. Rev. Lett.* 33:803–812.

Kuhlbrandt, W., and D. N. Wang. 1991. Three-dimensional structure of plant light-harvesting complex determined by electron crystallography. *Nature.* 350:130–135.

Kuhlbrandt, W., D. N. Wang, and Y. Fujiyoshi. 1994. Atomic model of plant light-harvesting complex by electron crystallography. *Nature.* 367: 614–621.

Pearlstein, R. M. 1982. Exciton migration and trapping in photosynthesis. *Photochem. Photobiol.* 35:835–844.

Porra, R. J., W. A. Thompson, and P. E. Kriedemann. 1989. Determination of accurate exctinction coefficient and simultaneous equations for assaying chlorophyll a and b extracted with four different solvent: verification of the concentration of chlorophyll standards by atomic absorption spectrometry. *Biochim. Biophys. Acta.* 975:384–394.

Press, W. H., B. P. Flannery, S. A. Teukolsky, and W. T. Vetterling. 1986. Numerical Recipes. Cambridge University Press, Cambridge.

Remelli, R., C. Varotto, D. Sandonà, R. Croce, and R. Bassi. 1999. Chlorophyll binding to monomeric light harvesting complex: a mutational analysis of chromophore binding residues. *J. Biol. Chem.* 274: 33510–33521.

Sandonà, D., R. Croce, A. Pagano, M. Crimi, and R. Bassi. 1998. Higher plant light harvesting proteins: structure and function as revealed by mutation analysis of either protein or cromophore moieties. *Biochim. Biophys. Acta.* 1365:207–214.

Seely, G. R., and R. G. Jensen. 1965. Effects of solvents on the spectrum of chlorophyll. *Spectrochim. Acta.* 21:1835–1845.

Shipman, L. L., and D. L. Hausmann. 1979. Förster transfer rate for chlorophyll a. *Photochem. Photobiol.* 29:1163–1167.

Simonetto, R., M. Crimi, D. Sandonà, R. Croce, G. Cinque, J. Breton, and R. Bassi. 1999. Orientation of chlorophyll transition moment in the higher plant light harvesting complex CP29. *Biochemistry.* 38: 12974–12983.

Stepanov, B. I. 1957. A universal relation between absorption and luminescence spectra of complex molecules. *Sov. Phys. Dokl.* 2:81–84.

Trinkunas, G., J. P. Connelly, M. G. Muller, L. Valkunas, and A. R. Holzwarth. 1997. Model for the excitation dynamics in the light-harvesting complex II from higher plants. *J. Phys. Chem* 101: 7313–7320.

van Grondelle, R. 1985. Excitation energy transfer, trapping and annihilation in photosynthetic systems. *Biochim. Biophys. Acta.* 811:147–195.

van Grondelle, R., J. P. Dekker, T. Gillbro, and V. Sundstrom. 1994. Energy transfer in photosynthesis. *Biochim Biophy. Acta.* 1187:1–65.

Van Gurp, M., H. van Langen, G. van Ginkel, and J. K. Levine. 1988. Molecular orientation of natural dye in ordered systems studied with polarized light. *J. Theor. Biol.* 131:333–349.

Visser, H. M., F. J. Kleima, R. van Stokkum, R. van Grondelle, and H. van Amerongen. 1996. Probing the many energy transfer processe in the photosystem light-harvestin complex II at 77 K using energy-selective sub-picosecond transient absorption spectroscopy. *Chem. Phys.* 210: 197–312.

Zucchelli, G., P. Dainese, R. C. Jennings, J. Breton, F. M. Garlaschi, and R. Bassi. 1994. Gaussian decomposition of absorption and linear dichroism spectra od outer antenna complexes of photosystem II. *Biochemistry.* 33:8982–8990.